Coherent destruction of tunneling of quantum energy transport in a driven nonequilibrium spin-boson model

Linlan Li and Xiufeng Cao*

Department of Physics, College of Physical Science and Technology, Xiamen University, Xiamen 361005, China

(Received 8 April 2024; revised 18 July 2024; accepted 22 July 2024; published 2 August 2024)

We investigate the steady-state energy flow of the periodically driven nonequilibrium spin-boson model by means of combining counter-rotating-hybridized rotating-wave (CHRW) method with full counting statistics. In the case of weak driving ($A < 0.1\Delta$), where A is the driving amplitude and Δ is the energy gap of the two-level system, our results are consistent with those obtained by traditional rotating-wave approximation (RWA) approach; in the case of high-frequency driving, our results are in agreement with the ones of the secular Floquet-Redfield method. As the driving amplitude increases, the steady-state flow exhibits nonlinear behavior: it reaches a maximum at medium driving, and then decreases to zero, which means that the coherent destruction of tunneling (CDT) appears, and then continues to grow slowly. We also find that, when the steady-state energy flow varies with driving frequency ω_d, comparing with RWA results, the counter-rotating (CR) terms increase the energy flow at low-frequency driving ($\omega_d < \Delta$), where ω_d is the driving frequency, and decreases it at high-frequency driving ($\omega_d > \Delta$). In the case of strong driving, when the zero-order Bessel function of the first kind satisfies $J_0(\frac{A}{\omega_d}\zeta) = 0$, instead of $J_0(\frac{A}{\omega_d}) = 0$, the steady-state energy flow is 0, which corresponds to the CDT of the energy flow. The modified parameter ζ mainly defines the contribution of the CR terms. At high-frequency driving, the modified parameter ζ tends to 1, our result is consistent with previous results $J_0(\frac{A}{\omega_d}) = 0$. We find that the CDT of flow only occurs when both CR terms of the driving and the dissipation are considered simultaneously. Our results show the influence of the CR terms on the energy flow and the modification of CDT condition and give theoretical guidance for energy transport of small quantum devices.

DOI: 10.1103/PhysRevB.110.075403

I. INTRODUCTION

Understanding and manipulating energy transport in low-dimensional materials is of great significance for scientific development and practical applications. The energy transport of nonequilibrium quantum systems has attracted great attention [1]. The nonequilibrium spin-boson (NESB) model, which is initially proposed by Segal and Nitzan [2,3], is considered as the most fundamental and commonly used model for studying quantum transport phenomenon. Technically, there are many methods to solve this model, such as noninteracting-blip approximation (NIBA) solving the dissipation dynamics of strong system-bath coupling [4–6], nonequilibrium Green's function (NEGF) method solving the dissipation dynamics [7], and Redfield scheme solving the dissipation dynamics of weak system-bath coupling [2,8]. In order to unify the description of the dynamics of the NESB, nonequilibrium polaron-transformed Redfield equation and polaron-transformed nonequilibrium Green function are proposed [9–11]. It should be noted that the nonequilibrium polaron transformation is reduced to NIBA once thermal baths are characterized as the Ohmic case. This limitation of the polaron transformation in handling Ohmic bath inspires to improve this transformation. Zheng's group propose an improved transformation: counter-rotating-hybridized rotating-wave method (CHRW) to investigate the equilibrium dynamics of driven two-level system [12–14]. This approach is beyond the traditional rotating-wave approximation (RWA) and allows to explore the effects of CR terms. In this paper, we extend the zero temperature CHRW to finite temperature systems and combine it with the full counting statistics to research the effects of CR terms on the energy transport of the driven-NESB model.

Recently, the driven-NESB model has been widely studied [15–17], in nanomaterials, such as superconducting devices based on Josephson tunneling junctions [18,19], optically and electrically controlled qubits in quantum dots [20–22], etc. The suitability of the Floquet theorem for the study of periodically driven systems has been extensively established [23–25]. In the driven-NESB model, the off-diagonal terms of the density matrix were usually omitted in the secular Floquet-Redfield method, for it was usually believed that they only take effect in short time behavior and do not affect the steady state. The steady-state result of the density matrix only retains the diagonal terms [23–25]. Our steady-state energy flow clearly contains diagonal and off-diagonal terms of the density matrix. Moreover, the influence of the nonvanishing off-diagonal terms increase with the temperature difference of the two baths [26]. In nonequilibrium systems, the omission of CR terms and secular approximation would lead to the neglect

*Contact author: xfcao@xmu.edu.cn

of the steady-state flow caused by interplay between CR terms of driving and dissipation [26].

The dynamics of open system with periodical driving exhibits coherent destruction of tunneling (CDT) [27,28], that is, due to the destructive interaction between dissipation dynamics and external periodic driving, the transition between two quantum states can be suppressed. And this situation only is observed when consider both CR terms of the driving and dissipation simultaneously [13]. This paper mainly answers the following questions: (1) is there a CDT in the energy transport of the driven-NESB model? (2) What is the effect of the CR terms on the energy flow of the driven-NESB model? First, we apply time-dependent unitary transformations on the time-dependent Hamiltonian, which include both the CR terms of the driving and dissipation coupling. Then in the rotating frame, we obtain the effective time-independent Hamiltonian. The CR terms not only renormalize the bare Hamiltonian of the system, but also modify the spectral density of the system-bath interaction, resulting in significant influence of the driving parameters on the steady-state energy flow. However, the interaction form of the system-bath after transformation is similar to that of RWA, which means the results of CHRW satisfy the second law of thermodynamics [29–31]. Our results are in agreement with two existing results: they are consistent with RWA results in the case of weak dissipation and weak driving, and they are consistent with those of secular Floquet-Redfield method in high-frequency strong driving [28]. We demonstrate the variation of energy flow from weak to strong driving, and show the energy flow before and after CDT. Considering the CR terms, the condition of CDT should be $J_0(\frac{A}{\omega_d}\zeta)=0$, instead of $J_0(\frac{A}{\omega_d})=0$, and the modified parameter ζ is determined by the CR terms. When the driving is high-frequency, the modified parameter ζ is approximately to $\zeta\approx 1$, and our results are in agreement with the existing ones, $J_0(\frac{A}{\omega_d})=0$. Moreover, we find that the steady-state energy flow is exactly 0 only when both the CR terms of the driving and dissipation are considered simultaneously.

This paper is organized as follows. In Sec. II, we introduce the Hamiltonian of the periodically driven-NESB model and derive the equation of motion by using CHRW and full-counting statistics. The steady-state energy flow for various driving amplitude A and driving frequency ω_d are presented and discussed in Sec. III. Finally, the conclusion is given in Sec. IV.

II. MODEL AND THEORY

We consider driven-NESB model, as shown in Fig. 1, which consists of a periodically driven two-level system coupled to two individual thermal baths at different temperatures. The Hamiltonian of the model reads ($\hbar=1, k_B=1$),

$$\begin{aligned}\hat{H}(t) &= -\frac{1}{2}[\Delta\hat{\sigma}_z + A\cos(\omega_d t)\hat{\sigma}_x] + \sum_{k;v=L,R}\omega_{k,v}\hat{b}^\dagger_{k,v}\hat{b}_{k,v}\\ &\quad+\frac{1}{2}\sum_{k;v=L,R} g_{k,v}(\hat{b}^\dagger_{k,v}+\hat{b}_{k,v})\hat{\sigma}_x\\ &= -\frac{1}{2}\Delta\hat{\sigma}_z - \frac{A}{4}(\hat{\sigma}_+ e^{-i\omega_d t}+\hat{\sigma}_- e^{i\omega_d t})\end{aligned}$$

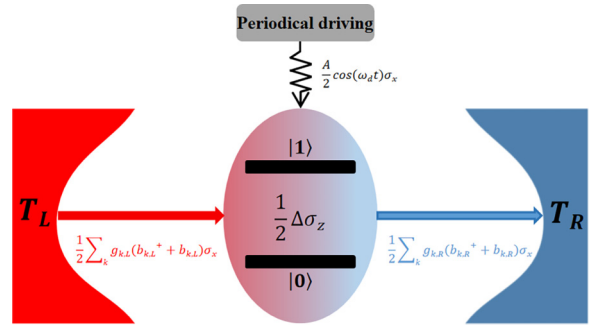

FIG. 1. Schematic description of the periodically driven nonequilibrium spin-boson model, composed by central periodically driven two-level system coupled to two individual thermal baths, with temperatures T_L and T_R, respectively. The red (blue) lines describe the interaction between the system and the Lth (Rth) bath.

$$\begin{aligned}&+\frac{1}{2}\sum_{k;v=L,R} g_{k,v}(\hat{b}^\dagger_{k,v}\hat{\sigma}_- + \hat{b}_{k,v}\hat{\sigma}_+)\\ &+\hat{H}_{\rm CR1}+\hat{H}_{\rm CR2}+\sum_{k;v=L,R}\omega_{k,v}\hat{b}^\dagger_{k,v}\hat{b}_{k,v},\end{aligned}\tag{1}$$

and both CR terms of driving and dissipation are

$$\hat{H}_{\rm CR1} = -\frac{A}{4}(\hat{\sigma}_+ e^{i\omega_d t}+\hat{\sigma}_- e^{-i\omega_d t}),\tag{2}$$

$$\hat{H}_{\rm CR2} = \frac{1}{2}\sum_{k;v=L,R} g_{k,v}(\hat{b}^\dagger_{k,v}\hat{\sigma}_+ + \hat{b}_{k,v}\hat{\sigma}_-),\tag{3}$$

where σ_μ ($\mu=x,y,z$) denote the μ-component Pauli matrix and $\sigma_\pm=(\sigma_x\pm i\sigma_y)/2$, Δ denotes the energy gap of the two-level system, and $A\cos(\omega_d t)$ is a time-dependent driving with the amplitude A and frequency ω_d. The bosonic operator $\hat{b}^\dagger_{k,v}(\hat{b}_{k,v})$ creates (annihilates) one phonon with energy $\omega_{k,v}$ and momentum k in the vth bath, and $g_{k,v}$ describes the coupling strength between the two-level system and the vth bath. Here, the vth bath is characterized by the spectral function as $G(\omega)=\sum_k g_k^2\delta(\omega-\omega_k)=2\alpha\omega\theta(\omega_c-\omega)$, where α is the dimensionless coupling constant, θ is the usual step function, and ω_c is the cutoff frequency. Note that, in the Hamiltonian, both the dissipation and the driving couple to σ_x and commute with each other. Usually, RWA neglects the CR terms $\hat{H}_{\rm CR1}$ and $\hat{H}_{\rm CR2}$, and is valid in the regime of weak driving and weak dissipation. In this work, we consider the influence of the CR terms of the driving and the dissipation on energy transport in a wide parameter range beyond weak driving.

The full counting statistics as a mathematically rigorous method is usually applied to measure the arbitrary order of the energy current fluctuation, of which the lowest order gives the energy flow. To calculate the energy flowing into the right bath, we include the auxiliary counting field χ to the whole Hamiltonian as $\hat{H}_\chi(t)=\exp(i\chi\sum_k\omega_{k,R}n_{k,R}/2)\hat{H}(t)\exp(-i\chi\sum_k\omega_{k,R}n_{k,R}/2)$ with $n_{k,R}=b^\dagger_{k,R}b_{k,R}$. When set $\chi=0$, the conventional Hamiltonian is recovered. The counting Hamiltonian is written as

$$\hat{H}_\chi(t)=\hat{H}_0(t)+\hat{H}_{1\chi},\tag{4}$$

with

$$\hat{H}_0(t) = -\frac{1}{2}[\Delta\hat{\sigma}_z + A\cos(\omega_d t)\hat{\sigma}_x] + \sum_{k;v=L,R}\omega_{k,v}\hat{b}^\dagger_{k,v}\hat{b}_{k,v} \quad (5)$$

and

$$\hat{H}_{1\chi} = \frac{1}{2}\sum_k g_{k,R}(b^\dagger_{k,R}e^{i\chi\omega_{k,R}/2} + b_{k,R}e^{-i\chi\omega_{k,R}/2})\hat{\sigma}_x + \frac{1}{2}\sum_k g_{k,L}(b^\dagger_{k,L} + b_{k,L})\hat{\sigma}_x. \quad (6)$$

In order to consider the CR terms, we apply the time-dependent canonical transformation [13] in the full counting statistics, $\hat{H}'(t) = e^{S(t)}\hat{H}_\chi(t)e^{-S(t)} - ie^{S(t)}\frac{d}{dt}e^{-S(t)}$. The generator of the unitary transformation is

$$S(t) = \left[-i\frac{A}{2\omega_d}\zeta\sin(\omega_d t) + \sum_k \frac{g_{k,L}}{2\omega_{k,L}}\xi_{k,L}(\hat{b}^\dagger_{k,L} - \hat{b}_{k,v}) + \sum_k \frac{g_{k,R}}{2\omega_{k,R}}\xi_{k,R}\left(\hat{b}^\dagger_{k,R}e^{\frac{i\chi\omega_{k,R}}{2}} - \hat{b}_{k,R}e^{\frac{-i\chi\omega_{k,R}}{2}}\right)\right]\sigma_x, \quad (7)$$

where we introduce two parameters of the transformation related to the driving and the dissipation, respectively, ζ and $\xi_{k,v}$. These parameters, $\zeta \in [0,1]$ and $\xi_{k,v} \in [0,1]$, which have value ranges from 0 to 1, determine the valid range of CHRW. And these parameters will be determined later. When $\xi_{k,v} = 0$ and $\zeta \neq 0$, the generator (7) becomes the one used for taking account of the CR terms of the driving. And when $\xi_{k,v} \neq 0$ and $\zeta = 0$, the generator (7) changes into the generator of treating the CR terms of dissipation. The details of CHRW are shown in Appendix A. After the transformation, the effective Hamiltonian is obtained in the first order approximation of $g_{k,v}$, $\hat{H}'(t) = \hat{H}'_0(t) + \hat{H}'_{1\chi}$, where the renormalized driven two-level system and first-order dissipation interaction terms are given by

$$\hat{H}'_0(t) = -\frac{1}{2}J_0\left(\frac{A}{\omega_d}\zeta\right)\eta\Delta\sigma_z + \sum_{k;v=L,R}\omega_{k,v}\hat{b}^\dagger_{k,v}\hat{b}_{k,v} - \frac{\tilde{A}}{4}(\sigma_+e^{-i\omega_d t} + \sigma_-e^{i\omega_d t}) \quad (8)$$

and

$$\hat{H}'_{1\chi} = \frac{1}{2}\sum_{k,v}\tilde{g}_{k,v}\left(\hat{b}^\dagger_{k,v}e^{\frac{i\chi\omega_{k,v}\delta_{v,R}}{2}}\sigma_- + \hat{b}_{k,v}e^{\frac{-i\chi\omega_{k,v}\delta_{v,R}}{2}}\sigma_+\right), \quad (9)$$

with the Kronecker delta $\delta_{v,R}$. If all subscripts are equal, $\delta_{v,R}$ is equal to 1, otherwise it is 0. And $\eta = \eta_R\eta_L$ with

$$\eta_v = \exp\left[-\sum_k \frac{2g^2_{k,v}}{\omega^2_{k,v}}\xi^2_{k,v}\coth\left(\frac{\omega_{k,v}}{2T_v}\right)\right]. \quad (10)$$

The coupling strength $\tilde{g}_{k,v}$ is modified by CR terms,

$$\tilde{g}_{k,v} = g_{k,v}\frac{2J_0\left(\frac{A}{\omega_d}\zeta\right)\eta_v\Delta}{\omega_{k,v} + J_0\left(\frac{A}{\omega_d}\zeta\right)\eta_v\Delta}. \quad (11)$$

To minimize the ground state energy of the system, two parameters $\xi_{k,v}$ and ζ are determined by the function,

$$\xi_{k,v} = \frac{\omega_{k,v}}{\omega_{k,v} + J_0\left(\frac{A}{\omega_d}\zeta\right)\eta_v\Delta} \quad (12)$$

and

$$J_1\left(\frac{A}{\omega_d}\zeta\right)\eta\Delta = \frac{1}{2}A(1-\zeta) \equiv \frac{\tilde{A}}{4}. \quad (13)$$

The parameters ζ and $\xi_{k,v}$ are uniquely determined by Eqs. (12) and (13). Meanwhile, the scope of the parameters, $\zeta \in [0,1]$ and $\xi_{k,v} \in [0,1]$ naturally provides the applicable conditions of CHRW. The self consistent solutions of Eqs. (12) and (13) are constrained by A, ω_d, and α. For high-frequency driving, this method works very well even if A/ω_d increases up to 6 [13].

Then, in the rotating frame of $\hat{H}'(t)$, $\tilde{H} = R(t)\hat{H}'(t)R^\dagger(t) - iR(t)\frac{d}{dt}R^\dagger(t)$ with the operator $R(t) = \exp[i\omega_d t(-\frac{1}{2}\sigma_z + \sum_{k,v} n_{k,v})]$, we obtain a time-independent Hamiltonian, $\tilde{H} = \tilde{H}_0 + \tilde{H}_{1\chi}$, where the bare Hamiltonian is

$$\tilde{H}_0 = -\frac{1}{2}\left(\tilde{\delta}\sigma_z + \frac{\tilde{A}}{2}\sigma_x\right) + \sum_{k,v}(\omega_{k,v} - \omega_d)b^\dagger_{k,v}b_{k,v}, \quad (14)$$

with the detuning $\tilde{\delta} = J_0(\frac{A}{\omega_d}\zeta)\eta\Delta - \omega_d$. The dissipation interaction is

$$\tilde{H}_{1\chi} = \frac{1}{2}\sum_{k,v}\tilde{g}_{k,v}(b^\dagger_{k,v}e^{i\chi\omega_{k,v}\delta_{v,R}/2}\sigma_+ + \text{H.c.}). \quad (15)$$

Here, we emphasize that the spectral density in transformed Hamiltonian is renormalized as

$$\tilde{G}(\omega) = \sum_k \tilde{g}^2_k\delta(\omega - \omega_k) = \left[\frac{2J_0\left(\frac{A}{\omega_d}\zeta\right)\eta_v\Delta}{\omega + J_0\left(\frac{A}{\omega_d}\zeta\right)\eta_v\Delta}\right]^2 G(\omega), \quad (16)$$

which is the result of the combination of the CR terms of the driving and the dissipation and also is the keypoint to CDT in the energy transport. We define a renormalization factor of correlation spectrum as, $F = \tilde{G}(\omega)/G(\omega) = [\frac{2J_0(\frac{A}{\omega_d}\zeta)\eta_v\Delta}{\omega + J_0(\frac{A}{\omega_d}\zeta)\eta_v\Delta}]^2$. For comparison, Table I shows the physical quantities modified by different CR terms, denoted by labels ζ-RWA, ξ_k-RWA, and ζ-ξ_k-RWA, respectively: that only involve the CR terms of the driving, that only involve the CR terms of the dissipation, and that involve both CR terms of the driving and dissipation.

Figure 2 shows the spectral density when different CR terms are considered. If only considering the CR terms of the driving, the spectral density that characterizes the dissipation from the bath is not renormalized. While considering CR term of the dissipation or both CR terms of the driving and the dissipation simultaneously, the spectral density is renormalized. That is, the renormalization of the spectral density is directly caused by CR term of the dissipation. Comparing the results of ξ_k-RWA and ζ-ξ_k-RWA, CR terms of the driving greatly reduce the spectral density. When adjust the driving amplitude A and frequency ω_d to achieve $J_0(\frac{A}{\omega_d}\zeta) = 0$, we see

TABLE I. The modified quantities of different CR terms.

	RWA	ζ-RWA	ξ_k-RWA	ζ-ξ_k-RWA
CR term of the driving		$\surd$		$\surd$
CR term of the dissipation			$\surd$	$\surd$
Driving amplitude	A	$\tilde{A}=4J_1\left(\frac{A}{\omega_d}\zeta\right)\Delta$	A	$\tilde{A}=4J_1\left(\frac{A}{\omega_d}\zeta\right)\eta\Delta$
Detuning δ	$\Delta-\omega_d$	$J_0\left(\frac{A}{\omega_d}\zeta\right)\Delta-\omega_d$	$\eta\Delta-\omega_d$	$J_0\left(\frac{A}{\omega_d}\zeta\right)\eta\Delta-\omega_d$
Coupling strength g_k	g_k	g_k	$\tilde{g}_k=\frac{2\eta\Delta}{\omega_k+\eta\Delta}g_k$	$\tilde{g}_k=\frac{2J_0(\frac{A}{\omega_d}\zeta)\eta\Delta}{\omega_k+J_0(\frac{A}{\omega_d}\zeta)\eta\Delta}g_k$
Spectral density $G(\omega)$	$G(\omega)$	$G(\omega)$	$\tilde{G}(\omega)=\left[\frac{2\eta\Delta}{\omega+\eta\Delta}\right]^2G(\omega)$	$\tilde{G}(\omega)=\left[\frac{2J_0(\frac{A}{\omega_d}\zeta)\eta\Delta}{\omega+J_0(\frac{A}{\omega_d}\zeta)\eta\Delta}\right]^2G(\omega)$

that the spectral density of ζ-ξ_k-RWA is 0, as shown in the Fig. 2(c). Meanwhile, the Hamiltonian of two-level system is zero, $H_{\rm TLS}=-\frac{1}{2}J_0(\frac{A}{\omega_d}\zeta)\eta\Delta\sigma_z=0$.

Then we derive the equation of motion combined with full counting statistics. In the interaction picture, the total density matrix of the system and bath, $\tilde{\rho}^I_{SB}(t)=e^{i\tilde{H}_0t}\tilde{\rho}_{SB}(t)e^{-i\tilde{H}_0t}$, satisfies the equation,

$$\frac{d}{dt}\tilde{\rho}^I_{SB}(\chi,t)=-i\big[\tilde{H}^I_1(\chi,t),\tilde{\rho}^I_{SB}(\chi,t)\big], \tag{17}$$

where superscript I indicates that the operator is in the interaction picture and $\tilde{H}^I_1(\chi,t)=e^{i\tilde{H}_0t}\tilde{H}_{1\chi}e^{-i\tilde{H}_0t}$. The relation with counting field χ is given as, $[A(\chi),B(\chi,t)]=A(\chi),B(\chi,t)-B(\chi,t)A(-\chi)$. The differential equation Eq. (17) can be integrated formally,

$$\tilde{\rho}^I_{SB}(\chi,t)=\tilde{\rho}^I_{SB}(\chi,0)-i\int_0^t d\tau\big[\tilde{H}^I_1(\chi,t),\tilde{\rho}^I_{SB}(\chi,\tau)\big]. \tag{18}$$

Substituting Eq. (18) into Eq. (17) and taking trace over two baths, the integrodifferential equation of reduced density matrix $\tilde{\rho}^I_S(\chi,t)=\mathrm{Tr_B}[\tilde{\rho}^I_{SB}(\chi,t)]$ is written as

$$\frac{d}{dt}\tilde{\rho}^I_S(\chi,t)=-i\int_0^t d\tau\mathrm{Tr_B}\big[\tilde{H}^I_1(\chi,t),\big[\tilde{H}^I_1(\chi,\tau),\tilde{\rho}^I_{SB}(\chi,\tau)\big]\big]. \tag{19}$$

In Born-Markov approximation, we obtain

$$\frac{d}{dt}\tilde{\rho}^I_S(\chi,t)=-i\int_0^\infty d\tau\mathrm{Tr_B}\big[\tilde{H}^I_1(\chi,t),\big[\tilde{H}^I_1(\chi,t-\tau),\tilde{\rho}^I_S(\chi,t)\rho_B\big]\big]. \tag{20}$$

After transforming the equation back into the Schrödinger picture and using the Kronecker product property and the technique of Lyapunov matrix equation, we expand the density matrix into a vector $|\tilde{\rho}_S(\chi,t)\rangle=|\tilde{\rho}_{11}(\chi,t),\tilde{\rho}_{12}(\chi,t),\tilde{\rho}_{21}(\chi,t),\tilde{\rho}_{22}(\chi,t)\rangle$. The equation of motion is expressed as

$$\frac{d}{dt}|\tilde{\rho}_S(\chi,t)\rangle=\hat{\mathcal{L}}(\chi)\tilde{\rho}_S(\chi,t)\rangle, \tag{21}$$

where $\hat{\mathcal{L}}(\chi)$ is the Liouvillion superoperator. The reduced density matrix is given by $\tilde{\rho}_S(\chi,t)=\exp[\hat{\mathcal{L}}(\chi)t]\tilde{\rho}_S(\chi,0)$, with the initial state $\tilde{\rho}_S(\chi,0)$. Therefore the cumulant generating function is obtained, $G_t(\chi)=\partial\ln\mathcal{Z}_\chi(t)/\partial t$, and the cumulant function is $\mathcal{Z}_\chi(t)=\mathrm{Tr_S}[\tilde{\rho}_S(\chi,t)]$. Then the corresponding nth cumulant of heat current fluctuations is given by $J^{(n)}(t)=\partial^n\ln G_t(\chi)/\partial(i\chi)^n|_{\chi=0}$. In particular, the energy flow is the first cumulant $J(t)=\partial\ln G_t(\chi)/\partial i\chi|_{\chi=0}$. The details of the derivation of the steady-state flow are given in Appendix B. The steady-state flow is written as

$$J_{ss}=\omega_1\gamma_{R,1}\frac{\sin^2(2\phi)}{2}[1-(2n_{R,1}+1)(\tilde{\rho}_{11}-\tilde{\rho}_{22})_{ss}]+\omega_1\gamma_{R,1}\frac{\sin(2\phi)\cos(2\phi)}{2}(2n_{R,1}+1)(\tilde{\rho}_{12}+\tilde{\rho}_{21})_{ss}$$

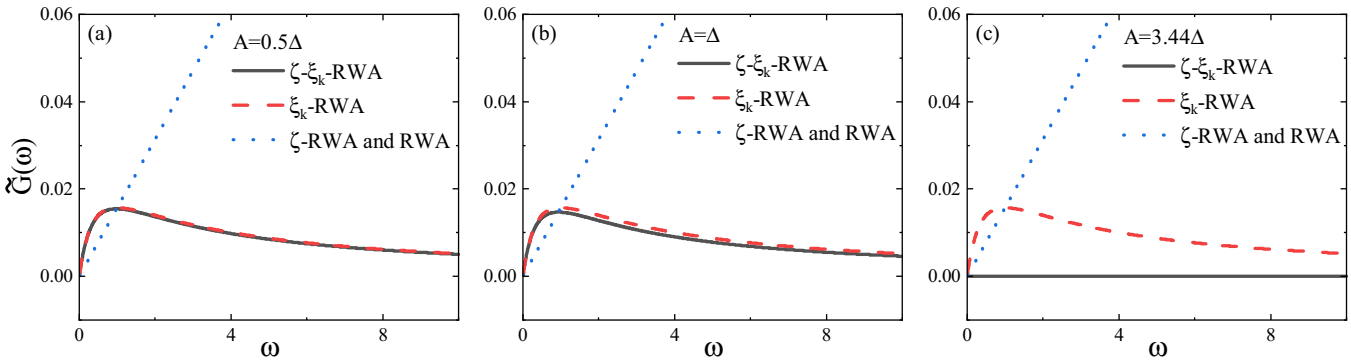

FIG. 2. Modified spectral density $G(\omega)$ as the function of frequency ω: (a) $A=0.5\Delta$, (b) Δ, and (c) 3.44Δ. The driving frequency $\omega_d=\Delta$.

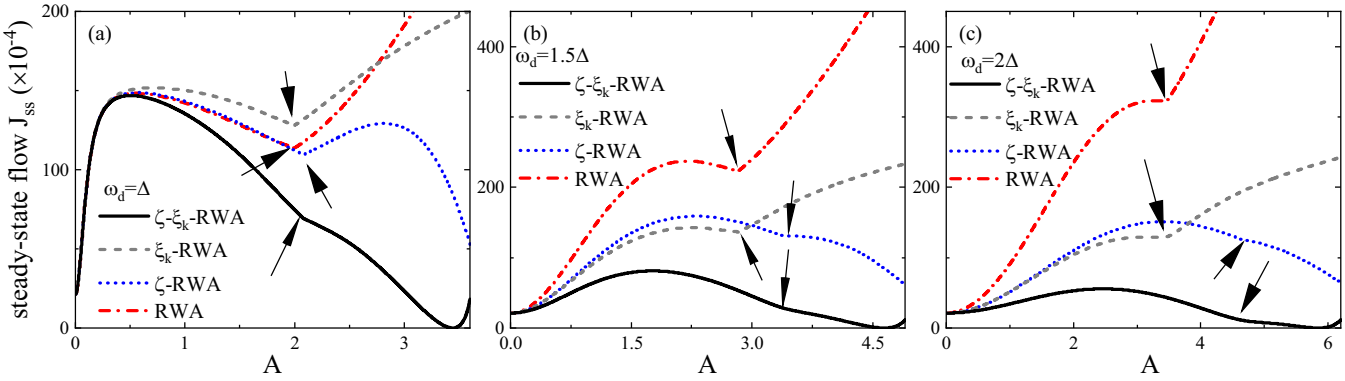

FIG. 3. The steady-state energy flow J_{ss} as the function of driving amplitude A for the four methods: (a) $\omega_d = \Delta$, (b) 1.5Δ, and (c) 2Δ. The temperatures of the baths are $T_L = 0.5\Delta$ and $T_R = 0.05\Delta$.

$$
\begin{aligned}
&+ \omega_2\gamma_{R,2}\cos^4(\phi)[1-(2n_{R,2}+1)(\tilde{\rho}_{11}-\tilde{\rho}_{22})_{ss}] \\
&- \omega_2\gamma_{R,2}\frac{\sin(2\phi)\cos^2(\phi)}{2}(2n_{R,2}+1)(\tilde{\rho}_{12}+\tilde{\rho}_{21})_{ss} \\
&+ \omega_3\gamma_{R,3}\sin^4(\phi)[1-(2n_{R,3}+1)(\tilde{\rho}_{11}-\tilde{\rho}_{22})_{ss}] \\
&+ \omega_3\gamma_{R,3}\frac{\sin(2\phi)\sin^2(\phi)}{2}(2n_{R,3}+1)(\tilde{\rho}_{12}+\tilde{\rho}_{21})_{ss},
\end{aligned}
\tag{22}
$$

where $\tilde{\rho}_{11}$ and $\tilde{\rho}_{22}$ are the diagonal terms of the density matrix, $\tilde{\rho}_{12}$ and $\tilde{\rho}_{21}$ are the off-diagonal terms; please see Appendix B for the definition of other parameters. The energy flow Eq. (22) clearly contains diagonal, $(\tilde{\rho}_{11}-\tilde{\rho}_{22})_{ss}$ and off-diagonal terms, $(\tilde{\rho}_{12}+\tilde{\rho}_{21})_{ss}$. The steady-state population difference $(\tilde{\rho}_{11}-\tilde{\rho}_{22})_{ss}$ is,

$$
(\tilde{\rho}_{11}-\tilde{\rho}_{22})_{ss} = \frac{4\gamma_e(\gamma_y\gamma_z+\tilde{\delta}^2)-4\gamma_c\gamma_d\gamma_y-2\tilde{A}\tilde{\delta}\gamma_d}{\tilde{A}^2\gamma_z-2\tilde{A}\tilde{\delta}\gamma_c+4\gamma_x(\gamma_y\gamma_z+\tilde{\delta}^2)}. \tag{23}
$$

And the steady-state quantum coherence $(\tilde{\rho}_{12}+\tilde{\rho}_{21})_{ss}$ is

$$
(\tilde{\rho}_{12}+\tilde{\rho}_{21})_{ss} = \frac{2\tilde{A}\tilde{\delta}\gamma_e-\tilde{A}^2\gamma_d-4\gamma_d\gamma_x\gamma_y}{\tilde{A}^2\gamma_z-2\tilde{A}\tilde{\delta}\gamma_c+4\gamma_x(\gamma_y\gamma_z+\tilde{\delta}^2)}, \tag{24}
$$

with the quasienergy $\pm\tilde{\Omega} = \pm\sqrt{\tilde{\delta}^2+\frac{\tilde{A}^2}{4}}$ and the other parameters in Appendix B. The steady-state flow J_{ss} obviously contains three frequencies: $\omega_1 = \omega_d$, $\omega_2 = \omega_d + \tilde{\Omega}$ and $\omega_3 = \omega_d - \tilde{\Omega}$, which correspond to Mollow triple peaks of the spectrum. The renormalization parameters clearly show the interplay effect of the CR terms of the dissipation and the driving on energy flow. In absence of the external driving ($A = 0$), our results reduced to the previous result [32]

$$
J = \frac{2\eta\Delta\gamma_R(\eta\Delta)\gamma_L(\eta\Delta)[n_L(\eta\Delta)-n_R(\eta\Delta)]}{[2n_R(\eta\Delta)+1]\gamma_R(\eta\Delta)+2n_L(\eta\Delta)+1]\gamma_L(\eta\Delta)}. \tag{25}
$$

Comparing the two results of with driving and without driving, Eqs. (22) and (25), under the external driving, the energy transport changes from one channel $\omega = \eta\Delta$ to three channels corresponding to the Mollow triplet $\omega_1 = \omega_d$, $\omega_2 = \omega_d + \tilde{\Omega}$ and $\omega_3 = \omega_d - \tilde{\Omega}$.

III. RESULTS AND DISCUSSION

In this section, we discuss the steady-state flow J_{ss} of the driven-NESB with various driving amplitudes and temperature biases and show the interplay effect of the driving and dissipation on energy transport. Set $\Delta = 1$ as the energy unit and the system-bath coupling strength $\alpha_L = \alpha_R = 0.01$.

Firstly, we compare the steady-state energy flow given by the four methods: ζ-ξ_k-RWA, ξ_k-RWA, ζ -RWA, and RWA to demonstrate the effects of two kinds of CR terms on the energy transport. The flow J_{ss} is plotted as a function of driving amplitude A with $\omega_d = \Delta$ in Fig. 3(a), $\omega_d = 1.5\Delta$ in Fig. 3(b), and $\omega_d = 2\Delta$ in Fig. 3(c). In resonant case $\omega_d = \Delta$ with weak driving case $A < 0.5\Delta$, four methods share the same results. As we know, RWA is valid for the resonance or near-resonance case in the regime of weak driving and weak dissipation. Our method, including two kinds of CR terms, can return to the RWA results in the weak driving and weak dissipation case. This consistency in the weak interaction is derived directly from the renormalized parameters. That is to say, in weak driving range $A < 0.5\Delta$, the renormalization factors of correlation spectrum is $F \approx 1$; the driving amplitude is $\tilde{A} \approx A$; and the detuning is $\tilde{\delta} \approx \delta$. Then the effect of the CR terms is weak enough to be ignored. Beyond the case of weak interactions, the effect of CR terms becomes important.

In Fig. 3, increasing the driving amplitude A away from weak driving and tuning the driving frequency away from resonance, the energy flows considering both CR terms are significantly lower than in the other three cases. In high-frequency regime, $\omega_d > \Delta$, the CR terms generally reduces the steady-state energy flow. The most significant behavior is that when both CR terms of driving and dissipation are included simultaneously, although there is a temperature bias between the left and right baths, the steady-state energy flow exhibits CDT, which means that the energy flow disappears at A and ω_d in a special ratio that satisfies $J_0(\frac{A}{\omega_d}\zeta) = 0$. In resonant case of Fig. 3(a), the steady-state energy flow is strictly zero with $A \approx 3.5$. When $A > 3.5$, the system exhibits finite steady-state flow. In the case of nonresonance, such as $\omega_d = 1.5\Delta$, $J_{ss} = 0$ with the driving amplitude $A \approx 4.5$ and $\omega_d = 2\Delta$, $J_{ss} = 0$ with $A \approx 5.8$. Table II shows the condition of the CDT corresponding to different driving frequencies and amplitude. Note that when only the CR terms of the driving

TABLE II. Coherent destruction of tunneling condition.

ω_d	A	ζ	$J_0\left(\frac{A}{\omega_d}\right)$	$J_0\left(\frac{A}{\omega_d}\zeta\right)$	CDT
Δ	2.4048Δ	0.5584	1.3×10^{-5}	0.5975	×
Δ	3.443Δ	0.6984	-0.3716	1.2×10^{-4}	√
6Δ	14.4288Δ	0.9234	1.3×10^{-5}	0.0989	×
6Δ	15.467Δ	0.9329	-0.0863	1.8×10^{-5}	√
10Δ	24.048Δ	0.9551	1.3×10^{-5}	0.0573	×
10Δ	25.086Δ	0.9586	-0.0526	4.2×10^{-5}	√
20Δ	48.096Δ	0.9779	1.3×10^{-5}	0.0279	×
20Δ	49.134Δ	0.9789	-0.0266	2.0×10^{-5}	√

are considered, the steady-state flow is greatly reduced but not exactly zero.

Besides CDT, Fig. 3 has another feature: the flow J_{ss} shows an inflection point, which are marked by arrows. Those inflection points concave downward and occur in the specific frequency of $\omega_d - \tilde{\Omega} = 0$. As we know, with the Rabi frequency increasing, the spectrum of resonance fluorescence of two-level system changes from a single peak to a Mollow triplet [12], i.e., the energy transmitted changes from one resonant frequency $\omega_1 = \omega_d$ to the triplet frequencies: $\omega_1 = \omega_d$, the blueshifted frequency $\omega_2 = \omega_d + \tilde{\Omega}$ and the redshifted frequency $\omega_3 = \omega_d - \tilde{\Omega}$. Fixed the driving frequency ω_d, the quasienergy $\tilde{\Omega}$ increases as the driving amplitude A, accordingly. When $\tilde{\Omega}$ increases to satisfy the condition $\omega_3 = \omega_d - \tilde{\Omega} = 0$, the frequency of the redshift phonon is zero. And the channel that emits phonons with the redshift frequency ω_3 is closed. The original flow with three frequencies, ω_1, ω_2, and ω_3 becomes two-channel transport with frequencies ω_1 and ω_2. Therefore the steady-state flow shows a concave inflection point. Since there is only one solution for the driving parameters corresponding to $\omega_3 = 0$, only one concave inflection point occurs. Continue to increase the driving amplitude, the frequency of the emitted photon changes from $\omega_d - \tilde{\Omega}$ to $\tilde{\Omega} - \omega_d$ [28].

Figure 4 shows the steady-state energy flow J_{ss} as a function of driving frequency ω_d for the four methods with $A = 0.2\Delta$ in (a), $A = 0.5\Delta$ in (b), and $A = \Delta$ in (c). In general, at a fixed driving amplitude, the steady-state energy flow is similar to the Lorentz line with driving frequency. The four curves basically overlap at $A = 0.2\Delta$ in Fig. 4(a), which reconfirms that the results of the four methods are consistent under the weak interaction condition. As the driving amplitude A increases from 0.2Δ to 0.5Δ, then to Δ, the difference of the four methods becomes greater. And the CR terms become non-negligible for $A > 0.5\Delta$. The steady-state flow J_{ss} is maximum at the frequency $\omega_d \approx \Delta$, so the energy transport is mainly caused by the resonance between the driving frequency of the external field and the energy gap of the two-level system. In Figs. 4(b) and 4(c), the maximum of the energy flow remains at the resonant frequency, $\omega_d \approx \Delta$. In high-frequency region, $\omega_d > \Delta$, the flow obtained by ζ -ξ_k-RWA, is significantly lower than the other three methods. In low-frequency region, $\omega_d < \Delta$, the flow obtained by method ζ-ξ_k-RWA is larger. This indicates the CR terms have opposite effects on the energy flow in the high- and low-frequency regions, similar to the effect of CR in the quantum Zeno effect [33]. The peak width of steady-state energy flow increases with the increase of driving amplitude.

Next, we give the results of ζ-ξ_k-RWA and consider the interplay effect of both CR terms of the driving and the dissipation, on J_{ss}. Figure 5 plot the steady-state flow J_{ss} with driving frequency ω_d for various of driving amplitude A with temperature bias in 5(a) and without temperature bias in 5(b). When the temperature bias is $T_R = 0.05\Delta$ and $T_L = 0.5\Delta$, the energy flow in the low frequency ($\omega_d < \Delta$) and high-frequency ($\omega_d > \Delta$) regions is obviously higher than that without temperature bias with $T_R = T_L = 0.5\Delta$ in 5(b). But near the resonance region $\omega_d \approx \Delta$, the temperature bias has little effect on the energy flow. As shown in Fig. 5(b), in the case of high frequency $\omega_d \gg \Delta$, the steady-state energy flow

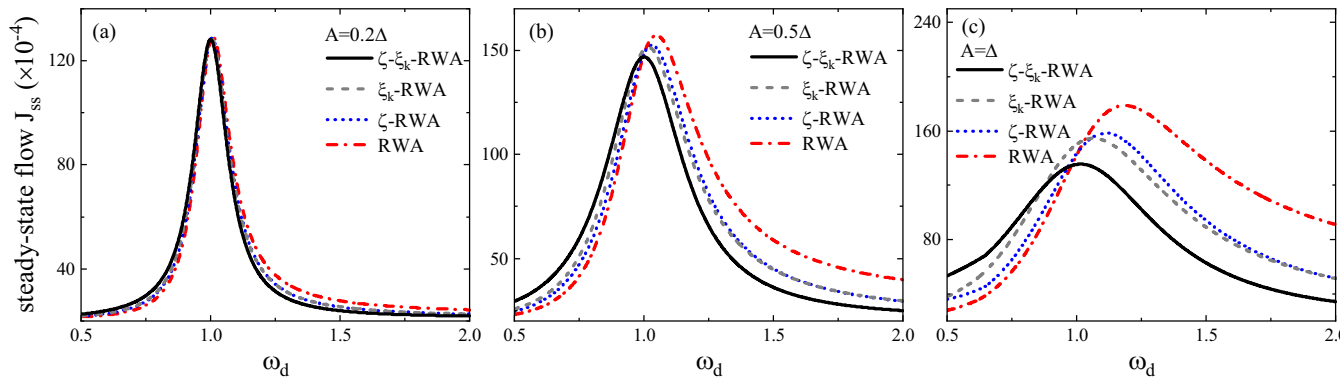

FIG. 4. The steady-state energy flow J_{ss} with driving frequency ω_d for the four methods: (a) $A = 0.2\Delta$, (b) 0.5Δ, and (c) Δ. The temperatures of the baths are $T_L = 0.5\Delta$ and $T_R = 0.05\Delta$.

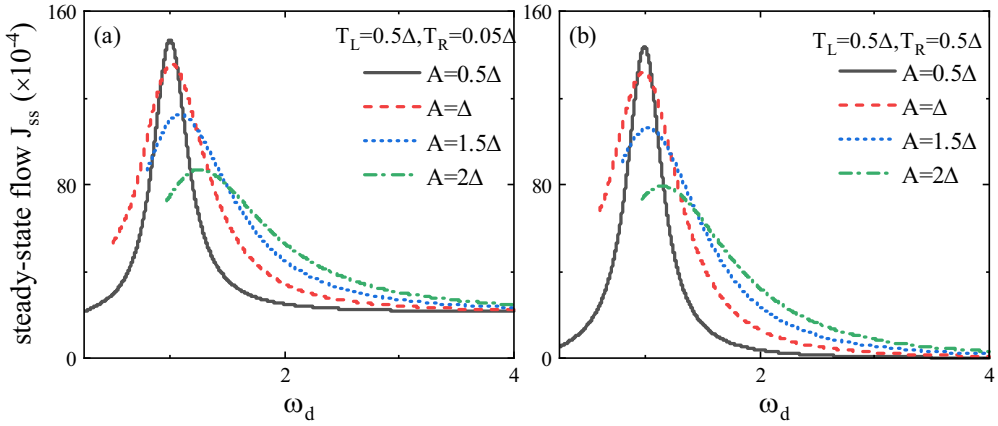

FIG. 5. The steady-state energy flow J_{ss} with driving frequency ω_d for various of the temperature bias and driving amplitude A: (a) $T_L = 0.5\Delta$, $T_R = 0.05\Delta$ and (b) $T_L = 0.5\Delta$, $T_R = 0.5\Delta$.

J_{ss} is almost zero without temperature bias. This indicates that when $\omega_d \gg \Delta$, the energy flow is mainly caused by temperature bias. Furthermore, when the driving amplitude A is less than Δ, the frequency corresponding to the maximum energy flow is approximately equal to energy gap of the two level system, $\omega_d \approx \Delta$. As driving amplitude A increases, regardless of whether there is a temperature bias between the two baths, the maximum steady-state energy flow decreases and the corresponding driving frequency moves towards higher frequency.

To further show the influence of driving and temperature bias on energy flow, we plot the steady-state flow J_{ss} with driving amplitude A for various temperature bias in resonance case $\omega_d = \Delta$ in Fig. 6(a), in nonresonance case $\omega_d = 5\Delta$ in Fig. 6(b) and $\omega_d = 10\Delta$ in Fig. 6(c). In Fig. 6(a), the energy flow is much larger than that in the case of nonresonance, and the influence of temperature bias is very small. Note the energy inflection points, which appears at $\omega_3 = \omega_d - \tilde{\Omega} = 0$, are more obvious in the low temperature region than in the high temperature region. In the conditions of large detuning in (b) and (c), the inflection point moves towards large driving amplitude. In the insets of Figs. 6(b) and 6(c), there are two inflection points: the first concave inflection point is $\omega_d - \tilde{\Omega} = 0$, which have discussed in Fig. 3; the second inflection point is $J_0(\frac{A}{\omega_d}\zeta) = 0$, which corresponds to CDT. The position of the inflection point of CDT is independent of the temperature of the two baths, which reflects the robustness of CDT to temperature bias. In flow J_{ss}, considering the CR terms, the CDT condition is $J_0(\frac{A}{\omega_d}\zeta) = 0$ instead of $J_0(\frac{A}{\omega_d}) = 0$. Table II gives the relationship between CDT and driving amplitude A and driving frequency ω_d. When the driving frequency is resonant to the energy gap of two-level system, the driving amplitude given by $J_0(\frac{A}{\omega_d}) = 0$ is $A = 2.4048\Delta$, and the driving amplitude of CDT given by our results is $A = 3.443\Delta$. The difference between the two driving amplitudes is mainly due to the influence of the CR terms in the strong driving case. In the resonance case with $A = 2.4048\Delta$, the renormalized parameter $\zeta = 0.5584$. Because the condition of CDT is always $A > 2\omega_d$, which has exceeded the applicable range of the RWA, so the research of the CDT have to consider the CR terms. And in the detuning case, the parameter ζ gradually approaches 1 as the driving frequency increases to more than 20Δ. Then, the CDT condition obtained by our method approaches the case of high-frequency strong driving, $J_0(\frac{A}{\omega_d}\zeta) \approx J_0(\frac{A}{\omega_d})$, which is based on the secular Floquet-Redfield formalism [28], as shown in Table II. In general, regardless of resonance or detuning, the study of CDT needs considering CR terms, instead of RWA.

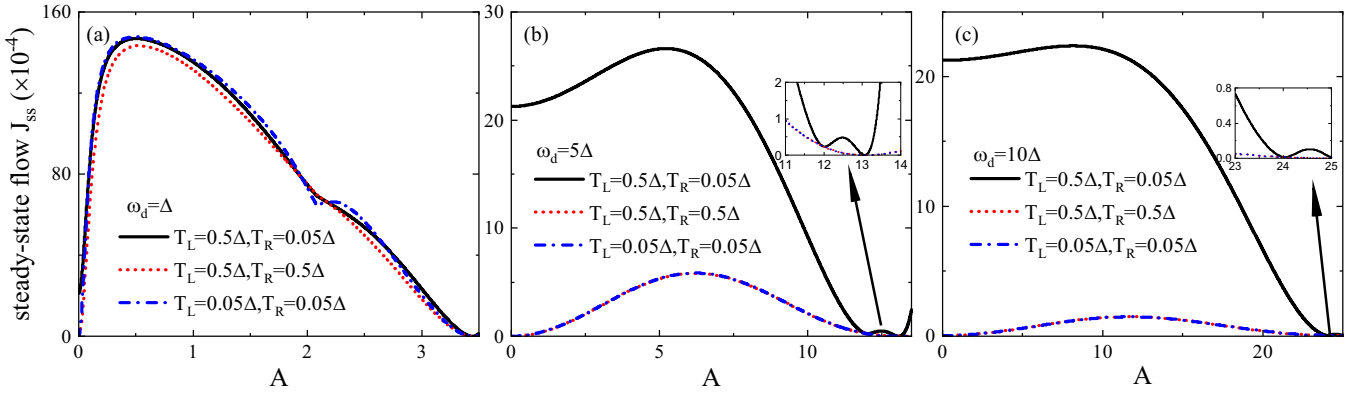

FIG. 6. The steady-state energy flow J_{ss} with driving amplitude A for various of the temperature bias and driving frequency ω_d: (a) Δ, (b) 5Δ, and (c) 10Δ. The insets are the magnifications of the energy flow near the inflection point and the CDT transition point.

IV. CONCLUSION

We study the steady-state energy flow J_{ss} of the periodically driven-NESB model combining CHRW transformations with full-counting statistics. Through the CHRW transformations, the effects of two types of CR terms (driving and dissipation) on the steady-state flow are considered. Our method is simple to analyze, and realizes the transition from strong driving to weak driving, and gives the steady-state energy flow caused by interplay between different CR terms. The flow J_{ss} under different CR terms, are consistent with the traditional RWA approach in weak driving and weak dissipation. However, as the driving amplitude increases, the influence of the CR terms on the energy flow becomes important and RWA is invalid. With the driving amplitude A from weak to strong, the steady-state flow J_{ss} shows nonmonotonic curves: firstly increases, and reaches the maximum value at the medium driving amplitude, and then decreases to zero, which corresponds to CDT, and then increases slowly. The CDT condition is $J_0(\frac{A}{\omega_d}\zeta)=0$, which differs from that of the high-frequency strong driving, $J_0(\frac{A}{\omega_d})=0$, mainly due to the renormalization coefficient ζ. This coefficient is $\zeta=0.5584$ in resonance and only approaches $\zeta=1$ at high-frequency, giving a result consistent with high-frequency based on secular Floquet-Redfield method. In addition, the CDT only occurs when both CR terms of the driving and the dissipation are considered simultaneously, and the position of the CDT does not depend on the temperature bias of the two baths. These results may deepen the understanding of nonequilibrium energy transport and the CDT effect in quantum transport and quantum thermodynamics. Moreover, it may provide theoretical guidance for the smart control of energy and information in low-dimensional quantum nanodevices.

ACKNOWLEDGMENT

X.-F.C. acknowledges support from the Fujian Province Natural Science Foundation under Grant No. 2022J01008.

APPENDIX A: THE UNITARY TRANSFORMATIONS

In this section, we describe in detail how to perform the CHRW transformation with the full counting statistics,

$$\hat{H}'(t)=e^{S(t)}\hat{H}_\chi(t)e^{-S(t)}-ie^{S(t)}\frac{d}{dt}e^{-S(t)} \tag{A1}$$

with the generator in Eq. (7). The transformed Hamiltonian is divided into three parts,

$$\hat{H}'(t)=\hat{H}'_0(t)+\hat{H}'_{1\chi}+\hat{H}'_2(t) \tag{A2}$$

with

$$\begin{aligned}\hat{H}'_0(t)=&-\frac{1}{2}J_0\Big(\frac{A}{\omega_d}\zeta\Big)\eta\Delta\sigma_z+J_1\Big(\frac{A}{\omega_d}\zeta\Big)\eta\Delta\sin(\omega_d t)\sigma_y\\&-\frac{A}{2}(1-\zeta)\cos(\omega_d t)\sigma_x+\sum_{k,v}\omega_{k,v}\hat{b}^\dagger_{k,v}b_{k,v}\\&+\sum_{k,v}\frac{g^2_{k,v}}{4\omega_{k,v}}\xi_{k,v}(\xi_{k,v}-2),\end{aligned} \tag{A3}$$

and

$$\begin{aligned}\hat{H}'_{I\chi}=&\frac{1}{2}J_0\Big(\frac{A}{\omega_d}\zeta\Big)\eta\Delta i\sigma_y X\\&+\frac{1}{2}\sigma_x\sum_{k,v}g_{k,v}(1-\xi_{k,v})\big(\hat{b}^\dagger_{k,v}e^{\frac{i\chi\omega_{k,v}\delta_{v,R}}{2}}+\text{H.c.}\big),\end{aligned} \tag{A4}$$

and

$$\begin{aligned}\hat{H}'_2(t)=&-\frac{1}{2}J_0\Big(\frac{A}{\omega_d}\zeta\Big)\Delta(\cosh X-\eta)\sigma_z\\&+\frac{1}{2}J_0\Big(\frac{A}{\omega_d}\zeta\Big)\Delta(\sinh X-\eta X)i\sigma_y\\&+J_1\Big(\frac{A}{\omega_d}\zeta\Big)\Delta(\cosh X-\eta)\sin(\omega_d t)\sigma_y\\&+iJ_1\Big(\frac{A}{\omega_d}\zeta\Big)\Delta\sinh X\sin(\omega_d t)\sigma_z\\&-\Delta(\cosh X\sigma_z-i\sinh X\sigma_y)\\&\times\sum_{n=1}^{\infty}J_{2n}\Big(\frac{A}{\omega_d}\zeta\Big)\cos(2n\omega_d t)\\&+\Delta(\cosh X\sigma_y+i\sinh X\sigma_z)\\&\times\sum_{n=1}^{\infty}J_{2n+1}\Big(\frac{A}{\omega_d}\zeta\Big)\cos[(2n+1)\omega_d t],\end{aligned} \tag{A5}$$

where $X=\sum_{k,v}\frac{g_{k,v}}{\omega_{k,v}}\xi_{k,v}(\hat{b}^\dagger_{k,v}e^{\frac{i\chi\omega_{k,v}\delta_{v,R}}{2}}+\hat{b}_{k,v}e^{\frac{-i\chi\omega_{k,v}\delta_{v,R}}{2}})$ and η in Eq. (10), the nth-order Bessel function of the first kind $J_n(z)$. In above derivation, we use the identity $\exp(iz\sin\alpha)=\sum_{n=-\infty}^{\infty}J_n(z)e^{in\alpha}$. And the parameter ζ is determined by Eq. (13). The Hamiltonian $\hat{H}'_0(t)$ is

$$\begin{aligned}\hat{H}'_0(t)=&-\frac{1}{2}J_0\Big(\frac{A}{\omega_d}\zeta\Big)\eta\Delta\sigma_z+\sum_{k;v=L,R}\omega_{k,v}\hat{b}^\dagger_{k,v}\hat{b}_{k,v}\\&-\frac{\tilde{A}}{4}(\sigma_+e^{-i\omega_d t}+\sigma_-e^{i\omega_d t}),\end{aligned} \tag{A6}$$

and the constant term is neglected. The second part $\hat{H}'_{1\chi}$ consist of the first order coupling of the system bath. Setting $\xi_{k,v}$ in the Eq. (12), the Hamiltonian $\hat{H}'_{I\chi}$ takes the RWA form

$$\hat{H}'_{1\chi}=\frac{1}{2}\sum_{k,v}\tilde{g}_{k,v}\big(\hat{b}^\dagger_{k,v}e^{\frac{i\chi\omega_{k,v}\delta_{v,R}}{2}}\sigma_-+\text{H.c.}\big), \tag{A7}$$

with a modified coupling strength

$$\tilde{g}_{k,v}=g_{k,v}\frac{2J_0\big(\frac{A}{\omega_d}\zeta\big)\eta_v\Delta}{\omega_{k,v}+J_0\big(\frac{A}{\omega_d}\zeta\big)\eta_v\Delta}. \tag{A8}$$

The modified correlation function of the system bath is much smaller and less than 0.02 as shown in Fig. 2. Therefore, under the transformed Hamiltonian, the equation of motion is safely approximates by the modified system-bath coupling coefficient. Since the effect of $\hat{H}'_2(t)$ on the dynamics is the fourth order of $\tilde{g}_{k,v}$, we ignore $\hat{H}'_2(t)$ in the derivation of equation of motion.

We simultaneously consider both CR terms of the dissipation and the driving and our results can easily fall back to

the case of only CR term of the driving or dissipation. Setting $\xi_{k,v} = 0$ in the unitary transformation, we obtain

$$\hat{H}'(t) = \hat{H}^{\zeta\text{-RWA}}(t) + \hat{H}'_2(t), \tag{A9}$$

with

$$\begin{aligned}\hat{H}^{\zeta\text{-RWA}}(t) = &-\frac{1}{2}J_0\left(\frac{A}{\omega_d}\zeta\right)\Delta\sigma_z + \sum_{k;v=L,R}\omega_{k,v}\hat{b}^\dagger_{k,v}\hat{b}_{k,v}\\ &-\frac{\tilde{A}}{4}(\sigma_+ e^{-i\omega_d t} + \sigma_- e^{i\omega_d t})\\ &+\frac{1}{2}\sum_{k,v} g_{k,v}\left(\hat{b}^\dagger_{k,v} e^{\frac{i\chi\omega_{k,v}\delta_{v,R}}{2}}\sigma_- + \text{H.c.}\right),\end{aligned} \tag{A10}$$

and

$$\begin{aligned}\hat{H}'_2(t) = &-\Delta\sum_{n=1}^{\infty}J_{2n}\left(\frac{A}{\omega_d}\zeta\right)\cos(2n\omega_d t)\sigma_z\\ &+\Delta\sum_{n=1}^{\infty}J_{2n+1}\left(\frac{A}{\omega_d}\zeta\right)\cos[(2n+1)\omega_d t]\sigma_y\\ &+\frac{1}{2}\sum_{k,v} g_{k,v}\left(\hat{b}^\dagger_{k,v} e^{\frac{i\chi\omega_{k,v}\delta_{v,R}}{2}}\sigma_+ + \text{H.c.}\right).\end{aligned} \tag{A11}$$

where the superscript ζ-RWA represents that the CR terms of the driving is involved and the CR terms of the dissipation are neglected. The parameters ζ and $\tilde{A}$ are obtained from Eq. (13) with $\eta = 1$. Setting $\zeta = 0$ in the unitary transformation, we obtain

$$\hat{H}'(t) = \hat{H}^{\xi_k\text{-RWA}}(t) + \hat{H}'_2(t), \tag{A12}$$

with

$$\begin{aligned}\hat{H}^{\xi_k\text{-RWA}}(t) = &-\frac{1}{2}\eta\Delta\sigma_z + \sum_{k;v=L,R}\omega_{k,v}\hat{b}^\dagger_{k,v}\hat{b}_{k,v}\\ &-\frac{A}{4}(\sigma_+ e^{-i\omega_d t} + \sigma_- e^{i\omega_d t})\\ &+\frac{1}{2}\sum_{k,v}\tilde{g}_{k,v}\left(\hat{b}^\dagger_{k,v} e^{\frac{i\chi\omega_{k,v}\delta_{v,R}}{2}}\sigma_- + \text{H.c.}\right),\end{aligned} \tag{A13}$$

and

$$\begin{aligned}\hat{H}'_2(t) = &-\frac{1}{2}\Delta(\cosh X - \eta)\sigma_z\\ &+\frac{1}{2}\Delta(\sinh X - \eta X)i\sigma_y\\ &-\frac{A}{4}(\sigma_- e^{-i\omega_d t} + \sigma_+ e^{i\omega_d t}),\end{aligned} \tag{A14}$$

where the superscript ξ_k-RWA represents that the CR terms of the dissipation are involved and the CR terms of the driving are neglected. The parameters η, $\xi_{k,v}$, and $\tilde{g}_{k,v}$ are obtained from Eqs. (10)–(12) with $J_0(\frac{A}{\omega_d}\zeta) = 1$.

APPENDIX B: THE DERIVATION OF STEADY-STATE ENERGY FLOW

This section provides the derivation of the equation of motion of the density matrix. Assuming two baths are thermal equilibrium, they follow the Bose-Einstein distribution that $\text{Tr}_B[\hat{b}^\dagger_{k,v}\hat{b}_{k,v}\rho_B] = n_{k,v}$ and $\text{Tr}_B[\hat{b}_{k,v}\hat{b}^\dagger_{k,v}\rho_B] = n_{k,v} + 1$ with $n_{k,v}$ the thermal average boson number at mode k given by $n_{k,v} = [\exp(\omega_k/k_B T_v) - 1]^{-1}$. According to Eqs. (A6) and (A7), we get the master equation in the Schrödinger picture,

$$\begin{aligned}\frac{d}{dt}\tilde{\rho}_s(\chi,t) = &-i[\tilde{H}_{os}, \tilde{\rho}_s(\chi,t)] - \int_0^\infty d\tau\frac{1}{4}\sum_{k,v}\tilde{g}^2_{k,v}[n_{k,v}\sigma_- e^{-i\tilde{H}_{os}\tau}\sigma_+ e^{i\tilde{H}_{os}\tau}\tilde{\rho}_s(t)e^{i(\omega_{k,v}-\omega_d)\tau}]\\ &-\int_0^\infty d\tau\frac{1}{4}\sum_{k,v}\tilde{g}^2_{k,v}[(n_{k,v}+1)\sigma_+ e^{-i\tilde{H}_{os}\tau}\sigma_- e^{i\tilde{H}_{os}\tau}\tilde{\rho}_s(\chi,t)e^{-i(\omega_{k,v}-\omega_d)\tau}]\\ &-\int_0^\infty d\tau\frac{1}{4}\sum_{k,v}\tilde{g}^2_{k,v}[(n_{k,v}+1)\tilde{\rho}_s(\chi,t)e^{-i\tilde{H}_{os}\tau}\sigma_+ e^{i\tilde{H}_{os}\tau}\sigma_- e^{i(\omega_{k,v}-\omega_d)\tau}]\\ &-\int_0^\infty d\tau\frac{1}{4}\sum_{k,v}\tilde{g}^2_{k,v}[n_{k,v}\tilde{\rho}_s(\chi,t)e^{-i\tilde{H}_{os}\tau}\sigma_- e^{i\tilde{H}_{os}\tau}\sigma_+ e^{-i(\omega_{k,v}-\omega_d)\tau}]\\ &+\int_0^\infty d\tau\frac{1}{4}\sum_{k,v}\tilde{g}^2_{k,v}[(n_{k,v}+1)e^{i\chi\omega_{k,v}\delta_{v,R}}\sigma_-\tilde{\rho}_s(\chi,t)e^{-i\tilde{H}_{os}\tau}\sigma_+ e^{i\tilde{H}_{os}\tau}e^{i(\omega_{k,v}-\omega_d)\tau}]\\ &+\int_0^\infty d\tau\frac{1}{4}\sum_{k,v}\tilde{g}^2_{k,v}[(n_{k,v}+1)e^{i\chi\omega_{k,v}\delta_{v,R}}e^{-i\tilde{H}_{os}\tau}\sigma_- e^{i\tilde{H}_{os}\tau}\tilde{\rho}_s(\chi,t)\sigma_+ e^{-i(\omega_{k,v}-\omega_d)\tau}]\\ &+\int_0^\infty d\tau\frac{1}{4}\sum_{k,v}\tilde{g}^2_{k,v}[n_{k,v}e^{-i\chi\omega_{k,v}\delta_{v,R}}\sigma_+\tilde{\rho}_s(\chi,t)e^{-i\tilde{H}_{os}\tau}\sigma_- e^{i\tilde{H}_{os}\tau}e^{-i(\omega_{k,v}-\omega_d)\tau}]\\ &+\int_0^\infty d\tau\frac{1}{4}\sum_{k,v}\tilde{g}^2_{k,v}[n_{k,v}e^{-i\chi\omega_{k,v}\delta_{v,R}}e^{-i\tilde{H}_{os}\tau}\sigma_+ e^{i\tilde{H}_{os}\tau}\tilde{\rho}_s(\chi,t)\sigma_- e^{i(\omega_{k,v}-\omega_d)\tau}].\end{aligned} \tag{B1}$$

Expand the density matrix $\tilde{\rho}_s(\chi,t)$ into a vector, $|\tilde{\rho}_S(\chi,t)\rangle = |\tilde{\rho}_{11}(\chi,t), \tilde{\rho}_{12}(\chi,t), \tilde{\rho}_{21}(\chi,t), \tilde{\rho}_{22}(\chi,t)\rangle$, and the equation of motion is expressed as

$$\frac{d}{dt}|\tilde{\rho}_S(\chi,t)\rangle = \hat{\mathcal{L}}(\chi)\tilde{\rho}_S(\chi,t)\rangle. \tag{B2}$$

Then we rotate the equation

$$U = \begin{pmatrix} 1 & 0 & 0 & 1 \\ 0 & 1 & 1 & 0 \\ 0 & 1 & -1 & 0 \\ 1 & 0 & 0 & -1 \end{pmatrix}. \tag{B3}$$

The rotated equation of motion is

$$\frac{d}{dt}|\tilde{\rho}'_S(\chi,t)\rangle = \hat{\mathcal{L}}'(\chi)|\tilde{\rho}'_S(\chi,t)\rangle, \tag{B4}$$

where $|\tilde{\rho}'_S(\chi,t)\rangle = |\tilde{\rho}_{S11}(\chi,t) + \tilde{\rho}_{S22}(\chi,t), \quad \tilde{\rho}_{S12}(\chi,t) + \tilde{\rho}_{S21}(\chi,t), \quad \tilde{\rho}_{S12}(\chi,t) - \tilde{\rho}_{S21}(\chi,t), \quad \tilde{\rho}_{S11}(\chi,t) - \tilde{\rho}_{S22}(\chi,t)\rangle$, and $\hat{\mathcal{L}}'(\chi) = U\hat{\mathcal{L}}(\chi)U^{-1}$. The steady-state cumulant generating function is derived as

$$\begin{aligned} J_{ss} &= \frac{\partial}{\partial(i\chi)}\left(\lim_{t\to\infty}\frac{\ln \mathcal{Z}_\chi(t)}{t}\right)\Big|_{\chi=0} \\ &= \lim_{t\to\infty}\frac{1}{t}\frac{\partial \ln \mathcal{Z}_\chi(t)}{\partial(i\chi)}\Big|_{\chi=0} \\ &= \langle I|\lim_{t\to\infty}\frac{1}{t}\frac{\partial\hat{\mathcal{L}}'(\chi)t}{\partial(i\chi)}\exp(\mathcal{L}'(\chi)t)|\tilde{\rho}'_S(\chi,0)\rangle|_{\chi=0}. \end{aligned} \tag{B5}$$

Then the steady-state solution of energy flow is simplified to

$$J_{ss} = \langle I|\frac{\partial\hat{\mathcal{L}}'(\chi)}{\partial(i\chi)}|_{\chi=0}|\tilde{\rho}'_S(t)\rangle_{ss}, \tag{B6}$$

with the steady-state density matrix $|\tilde{\rho}'_S(t)\rangle_{ss} = \lim_{t\to\infty}\exp(\hat{\mathcal{L}}'(\chi)t)\tilde{\rho}'_S(\chi,0)\rangle$. Put the matrix element of the superoperator $\hat{\mathcal{L}}'(\chi)$ into J_{ss}, the steady-state energy flow is written as

$$\begin{aligned} J_{ss} = &\frac{\partial[\hat{\mathcal{L}}_{14}(\chi)+\hat{\mathcal{L}}_{41}(\chi)]}{2\partial(i\chi)}\Big|_{\chi=0} \\ &+\frac{\partial[\hat{\mathcal{L}}_{12}(\chi)+\hat{\mathcal{L}}_{42}(\chi)]}{\partial(i\chi)}\Big|_{\chi=0}(\tilde{\rho}_{12}+\tilde{\rho}_{21})_{ss} \\ &+\frac{\partial[-\hat{\mathcal{L}}_{14}(\chi)+\hat{\mathcal{L}}_{41}(\chi)]}{2\partial(i\chi)}\Big|_{\chi=0}(\tilde{\rho}_{11}-\tilde{\rho}_{22})_{ss}, \end{aligned} \tag{B7}$$

with

$$\begin{aligned} &\frac{\partial}{\partial(i\chi)}\frac{[\hat{\mathcal{L}}_{14}(\chi)+\hat{\mathcal{L}}_{41}(\chi)]}{2}\Big|_{\chi=0} \\ &= \frac{\sin^2(2\phi)}{2}\omega_1\gamma_{R,1} + \cos^4(\phi)\omega_2\gamma_{R,2} \\ &\quad + \sin^4(\phi)\omega_3\gamma_{R,3}, \end{aligned} \tag{B8}$$

and

$$\begin{aligned} &\frac{\partial[\hat{\mathcal{L}}_{12}(\chi)+\hat{\mathcal{L}}_{42}(\chi)]}{\partial(i\chi)}\Big|_{\chi=0} \\ &= \frac{\sin(2\phi)\cos(2\phi)}{2}\omega_1\gamma_{R,1}(2n_{R,1}+1) \\ &\quad - \frac{\sin(2\phi)\cos^2(\phi)}{2}\omega_2\gamma_{R,2}(2n_{R,2}+1) \\ &\quad + \frac{\sin(2\phi)\sin^2(\phi)}{2}\omega_3\gamma_{R,3}(2n_{R,3}+1), \end{aligned} \tag{B9}$$

and

$$\begin{aligned} &\frac{\partial}{\partial(i\chi)}\frac{[-\hat{\mathcal{L}}_{14}(\chi)+\hat{\mathcal{L}}_{41}(\chi)]}{2}\Big|_{\chi=0} \\ &= -\frac{\sin^2(2\phi)}{2}\omega_1\gamma_{R,1}(2n_{R,1}+1) \\ &\quad - \cos^4(\phi)\omega_2\gamma_{R,2}(2n_{R,2}+1) \\ &\quad - \sin^4(\phi)\omega_3\gamma_{R,3}(2n_{R,3}+1). \end{aligned} \tag{B10}$$

The expression $(\tilde{\rho}_{11}-\tilde{\rho}_{22})_{ss}$ is the steady-state population difference, given in Eq. (23), and $(\tilde{\rho}_{12}+\tilde{\rho}_{21})_{ss}$ is the steady-state quantum coherence, shown in Eq. (24). The parameters of the steady-state energy flow J_{ss} in Eq. (22) are defined as $\gamma_x = \gamma_y + \gamma_z$ with $\cos^2(\phi) = \frac{1}{2}(1+\frac{\tilde{\delta}}{\tilde{\Omega}})$, $\gamma_y = \sin^2(2\phi)\Gamma_1 - \sin^2(\phi)\cos(2\phi)\Gamma_3 + \cos^2(\phi)\cos(2\phi)\Gamma_2$ and $\gamma_z = \sin^2\Gamma_3 + \cos^2(\phi)\Gamma_2$. The other variables are defined as follows: $\gamma_d = \sin(2\phi)\cos(2\phi)\gamma_1 + \sin^2(\phi)\sin(2\phi)\gamma_3 - \cos^2(\phi)\sin(2\phi)\gamma_2$, $\gamma_c = \sin(2\phi)\cos(2\phi)\Gamma_1 + \sin^2(\phi)\sin(2\phi)\Gamma_3 - \cos^2(\phi)\sin(2\phi)\Gamma_2$, and $\gamma_e = \sin^2(2\phi)\gamma_1 + 2\sin^4(\phi)\gamma_3 + 2\cos^4(\phi)\gamma_2$. And the finite temperature decay rate is $\Gamma_i = \sum_{v=L,R}(2n_{v,i}+1)\gamma_{v,i}$ and the zero temperature decay rate is $\gamma_i = \sum_{v=L,R}\gamma_{v,i}$ with $\gamma_{v,i} = \frac{\pi}{4}\sum_k \tilde{g}_{k,v}\delta(\omega-\omega_{k,v}) = \frac{\pi\tilde{G}_v(\omega_i)}{4}$. The energies with the subscripts $\omega_i\,(i=1,2,3)$ are denoted as respectively, $\omega_1 = \omega_d$, $\omega_2 = \omega_d + \tilde{\Omega}$, and $\omega_3 = \omega_d - \tilde{\Omega}$, which are concerned with Mollow triplet.

[1] G. Chen, *Nanoscale Energy Transport and Conversion: A Parallel Treatment of Electrons, Molecules, Phonons, and Photons* (Oxford University Press, Oxford, England, 2005).

[2] D. Segal and A. Nitzan, Phys. Rev. Lett. **94**, 034301 (2005).

[3] D. Segal, Phys. Rev. Lett. **101**, 260601 (2008).

[4] D. Segal, Phys. Rev. B **73**, 205415 (2006).

[5] L. Nicolin and D. Segal, J. Chem. Phys. **135**, 164106 (2011).

[6] T. Chen, X.-B. Wang, and J. Ren, Phys. Rev. B **87**, 144303 (2013).

[7] P. Portugal, C. Flindt, and N. Lo Gullo, Phys. Rev. B **104**, 205420 (2021).

[8] J. Ren, P. Hänggi, and B. Li, Phys. Rev. Lett. **104**, 170601 (2010).

[9] C. Wang, J. Ren, and J. Cao, Phys. Rev. A **95**, 023610 (2017).

[10] C. Wang, J. Ren, and J. Cao, Sci. Rep. **5**, 11787 (2015).

[11] J. Liu, H. Xu, B. Li, and C. Wu, Phys. Rev. E **96**, 012135 (2017).

[12] Y. Yan, Z. Lü, and H. Zheng, Phys. Rev. A **88**, 053821 (2013).

[13] Y. Yan, Z. Lü, and H. Zheng, Phys. Rev. A **90**, 053850 (2014).

[14] Z. Lü and H. Zheng, Phys. Rev. A **86**, 023831 (2012).
[15] D. Gelbwaser-Klimovsky and A. Aspuru-Guzik, J. Phys. Chem. Lett. **6**, 3477 (2015).
[16] S. Restrepo, J. Cerrillo, P. Strasberg, and G. Schaller, New J. Phys. **20**, 053063 (2018).
[17] C. Elouard, D. Herrera-Martí, M. Esposito, and A. Auffèves, New J. Phys. **22**, 103039 (2020).
[18] M. Hofheinz, H. Wang, M. Ansmann, R. C. Bialczak, E. Lucero, M. Neeley, A. D. O'Connell, D. Sank, J. Wenner, J. M. Martinis, and A. N. Cleland, Nature (London) **459**, 546 (2009).
[19] J. M. Martinis, M. H. Devoret, and J. Clarke, Nat. Phys. **16**, 234 (2020).
[20] J. Gorman, D. G. Hasko, and D. A. Williams, Phys. Rev. Lett. **95**, 090502 (2005).
[21] J.-H. Jiang, M. Kulkarni, D. Segal, and Y. Imry, Phys. Rev. B **92**, 045309 (2015).
[22] J. Ren, Chin. Phys. Lett. **40**, 090501 (2023).
[23] K. Szczygielski, D. Gelbwaser-Klimovsky, and R. Alicki, Phys. Rev. E **87**, 012120 (2013).
[24] D. Gelbwaser-Klimovsky, R. Alicki, and G. Kurizki, Phys. Rev. E **87**, 012140 (2013).
[25] R. Alicki and D. Gelbwaser-Klimovsky, New J. Phys. **17**, 115012 (2015).
[26] X. Cao, C. Wang, and D. He, Phys. Rev. B **108**, 245401 (2023).
[27] F. Grossmann, T. Dittrich, P. Jung, and P. Hänggi, Phys. Rev. Lett. **67**, 516 (1991).
[28] G. Engelhardt, G. Platero, and J. Cao, Phys. Rev. Lett. **123**, 120602 (2019).
[29] S. Gasparinetti, P. Solinas, A. Braggio, and M. Sassetti, New J. Phys. **16**, 115001 (2014).
[30] P. Wollfarth, A. Shnirman, and Y. Utsumi, Phys. Rev. B **90**, 165411 (2014).
[31] P. Wollfarth, Y. Utsumi, and A. Shnirman, Phys. Rev. B **96**, 064302 (2017).
[32] X. Cao, C. Wang, H. Zheng, and D. He, Phys. Rev. B **103**, 075407 (2021).
[33] H. Zheng, S. Y. Zhu, and M. S. Zubairy, Phys. Rev. Lett. **101**, 200404 (2008).